J Mol Model (2012) 18:2349–2356
DOI 10.1007/s00894-011-1253-7

ORIGINAL PAPER

Molecular simulation of water removal from simple gases with zeolite NaA

Éva Csányi · Zoltán Ható · Tamás Kristóf

Received: 12 August 2011 / Accepted: 21 September 2011 / Published online: 8 October 2011

Abstract Water vapor removal from some simple gases using zeolite NaA was studied by molecular simulation. The equilibrium adsorption properties of H_2O, CO, H_2, CH_4 and their mixtures in dehydrated zeolite NaA were computed by grand canonical Monte Carlo simulations. The simulations employed Lennard-Jones + Coulomb type effective pair potential models, which are suitable for the reproduction of thermodynamic properties of pure substances. Based on the comparison of the simulation results with experimental data for single-component adsorption at different temperatures and pressures, a modified interaction potential model for the zeolite is proposed. In the adsorption simulations with mixtures presented here, zeolite exhibits extremely high selectivity of water to the investigated weakly polar/non-polar gases demonstrating the excellent dehydration ability of zeolite NaA in engineering applications.

Keywords Zeolite · Selectivity · Dehydration · Simple gas mixture · Molecular simulation

Introduction

Zeolites consist of silicon-aluminium-oxygen networks with structurally well-defined pores. The high regularity of the structure distinguishes zeolites from other porous materials and makes their high selectivity in separation and catalytic processes possible [1, 2]. The advantage of zeolite membranes over other types of membranes is that they can tolerate high temperatures and harsh chemical environments. Zeolite NaA is a synthetic zeolite with small pores, and it is known to be outstanding for use in organic solvent dehydration due to its high hydrophilicity. In the past decade the separation and adsorption properties of zeolite NaA have been examined in several experimental studies [3–5], among others in connection with Fischer-Tropsch synthesis (FTS) technology [6]. FTS has gained current interest as an economic technology alternative to obtain liquid fuels from natural gas [7]. The raw synthesis gas of FTS, which can come from coal or biomass gasification, is a mixture of CO, CO_2, H_2, CH_4, etc., and water is also one of the products (e.g., over cobalt catalysts, generally one molecule H_2O produced for each CO molecule converted at temperatures between 473 and 523 K). However, water decreases the FTS reaction rate by deactivating a fraction of the catalyst grains, so its removal from the reaction mixture can enhance reactor efficiency.

The performance of zeolite NaA as a drying agent can, in principle, be determined experimentally. Another way to collect information is a theoretical approach such as molecular simulation [8]. Recently, we have studied the adsorption characteristics of zeolite NaA by Monte Carlo (MC) simulations [9–11]. We used several force fields for this zeolite—some developed by ourselves [10, 11], with others taken from the literature [12–14]. However, none of the models used proved to be entirely satisfactory. The first model [12] we used in our alcohol–water separation studies predicted too high equilibrium loadings for pure methanol and ethanol compared to the corresponding experimental data [3]. To correct this weakness, we developed a new model [10] keeping the semi-flexible concept. This model showed better agreement with the experimental data for the loadings of water, methanol and

É. Csányi · Z. Ható · T. Kristóf (✉)
Institute of Chemistry, Department of Physical Chemistry,
University of Pannonia,
P.O. Box 158, 8201 Veszprém, Hungary
e-mail: kristoft@almos.uni-pannon.hu

ethanol. The selectivity of water to alcohols was predicted to be higher. The main advantage of this model is that its parameters can be applied to zeolite NaA with other Si:Al ratios, since the charge parameter of Na^+ ions (charge compensation ions) was set to be equal to the difference between the charge parameters of Si and Al atoms. With this model, however, the experimental equilibrium loadings of non-polar gases were underestimated significantly. After optimizing parameters with the help of quantum chemical methods, we published a new zeolite model [11]. Nevertheless, to be able to provide reliable results on the selectivity of adsorption of water with respect to weakly polar or non-polar molecules like CO, H_2 and CH_4, we found it necessary to improve our new zeolite model even further.

In this paper, we investigate the selectivity of zeolite NaA in atomic detail, and present simulation results for the pressure and temperature dependencies of the adsorption from two-, three-, and four-component mixtures of H_2O, CO, H_2, and CH_4.

Methods

Models and model development

Zeolite NaA is of framework type LTA and has three kinds of rings (4R, 6R and 8R) containing four, six and eight O atoms, respectively. The interconnection of 4R and 6R rings forms nearly spherical cages called sodalite cages. The O bridges connect the sodalite cages to each other so that they form supercages with a diameter of about 1.2 nm. The crystal structure of zeolite NaA belongs to the fm-3c space group with a lattice parameter of 2.4555 nm. [15]

The unit cell composition of the crystal for the present study was chosen so that the Si/Al ratio was 1.0. The model of the zeolite consists of 576 framework atoms (96 Si, 96 Al, and 384 O atoms), where each AlO_4 tetrahedron is connected to a SiO_4 tetrahedron (according to the Löwenstein rule that prohibits Al–O–Al linkages). The potential model is defined by the positions of the interaction sites and their potential parameters, which are in this case Lennard-Jones energy (ε) and size (σ) parameters and point charges (q). Our model is semi-flexible, i.e., the framework atoms are fixed at the atomic positions taken from X-ray diffraction experiments [15] and all the 96 non-framework Na^+ ions are allowed to move.

During the development of the potential model we kept the rigid concept of the zeolite framework with mobile Na^+ cations by assuming only one type of structural O atom. In order to improve the transferability of the model, we first set the charge parameter of the Na^+ ions to 1 [10] and performed optimizations for the adsorption loadings both for water and simple alcohols (methanol and ethanol). Subsequent quantum chemical calculations suggested, however, that the model became excessively polar. Considering also the results of structure examinations by MC, we proposed recently a new parameter set for the model by lowering the charge parameter of the Na^+ ion [11]. The new model (in the following, model 3) provides a reasonably good reproduction of the experimental loadings for water, methanol, and ethanol at T=298 K. For carbon monoxide, however, we realized that this model still overestimates the available experimental data at T=373 K. As the charge parameter of the Na^+ ion primarily determines the polarity of the model, we tested some new values for this parameter and found that a slightly smaller value was suitable to reproduce satisfactorily the experimental data for both water and carbon monoxide. Table 1 lists the potential parameters of the models tested in this work.

In the simulations, we employed site–site (or all-atom) potential models for the adsorbates, because of their realistic, built-in electrostatic, dipole or quadrupole, moments. We used the SPC/E [16] model for water, the SK model [17] for carbon monoxide, the model proposed by Darkrim et al. [18] for hydrogen, and an OPLS-AA [19] model for methane. These models are known to be appropriate for the reproduction of thermodynamic properties of pure substances.

Lennard-Jones parameters between unlike interaction sites were calculated generally by the Lorentz-Berthelot combining rules. The only exception was the case of methane, because the literature OPLS-AA model fails to reproduce accurately the experimental thermodynamic data

Table 1 Lennard-Jones energy (ε) and size parameters (σ) and partial charges (q) for different models of zeolite NaA. Model 1 (M1) is taken from [14], model 2 (M2) is taken from [13], and model 3 (M3) is our previous model [11] (modified parameters in parentheses). The atomic positions of the zeolite framework are unchanged [15]

Sites	Na^+			O			Si			Al		
	M1	M2	M3	M1	M2	M3	M1	M2	M3	M1	M2	M3
(ε/k) / K	2137	8.0	100	83.4	22.0	200	-	-	-	-	-	-
σ / nm	0.172	0.285	0.25	0.32	0.3	0.33	-	-	-	-	-	-
q / electron charge	1.0	0.74	0.7 (0.6)	−1.2	−0.7	−1.2	2.05	0.8	2.4	1.75	1.42	1.7 (1.8)

of the fluid. This discrepancy is not specific to the choice of OPLS-AA potentials, but is rather linked to the occasional failure of the geometric mean combining rule to compute unlike atom interactions. Song et al. [20] found that the special character of methane interactions is not captured if standard combining rules are used, at least with the Lennard-Jones type pair potentials of the OPLS-AA model. They tested a number of alternative two-parameter combining rules, and concluded that alkane interactions can be described accurately by the combining rules proposed by Waldman and Hagler [21]. Following Song et al. [20], we used the Waldman-Hagler rules for the unlike interactions involving methane sites. The method links the behavior of ε_{ij} to the relative sizes of atoms i and j and provides smaller values for the unlike parameters when $\sigma_{ii} \neq \sigma_{jj}$.

Simulation details

Molecular simulations of adsorption were carried out using the grand canonical MC method [22]. The partial pressure values of the adsorbate molecules in the gas phase were given indirectly by specifying the component's chemical potential, which was calculated from the ideal gas law. The suitability of the ideal gas law was verified by test simulations in our earlier work [10]. The Wolf method [23, 24] was used to treat the Coulomb interactions with a convergence (damping) parameter of $\alpha = 2/r_c$ and cut-off radius of $r_c = L/2$ (where L is the length of the simulation box and is equal to the lattice parameter).

The grand canonical MC simulations with pure components consisted of an equilibration period (at least 10^8 MC moves) and a subsequent averaging period (at least 4×10^8 MC moves), where the ratio of insertion/deletion steps was 70–80%. In mixture simulations the sampling efficiency was increased by identity change attempts [25]. The creation of molecules inside the sodalite cages was prevented artificially by placing purely repulsive dummy atoms at the center of these cages because the standard random insertion of molecules cannot take into account the physical diffusion pathways in the zeolite. The accessibility of the sodalite cages for adsorbate molecules is still an open question, about which there is some disagreement in the literature [8, 26]. Sodalite cages are very probably not accessible for larger molecules like CO or CH_4. However, H_2 is small enough to pass through the windows of the sodalite cages. We tested both cases for H_2, and found that the experimental adsorption coverages are slightly underestimated when insertion into sodalite cages is prevented, while these data are overestimated by the same extent when the insertion is permitted. With our choice of blocking the creation of hydrogen in sodalite cages, we kept a uniform concept for our adsorption simulations, which probably produced only small errors in the results (the transition of molecules into sodalite cages with translational moves was not forbidden).

In the grand canonical simulation, besides the adsorption loading, we also calculated the isosteric heat of adsorption using the following expression:

$$q_{st,i} = \left(\frac{\partial H^b}{\partial n_i^b}\right)_{p,T,n_{i\neq j}} - \left(\frac{\partial U^a}{\partial n_i^a}\right)_{V,T,n_{i\neq j}},$$

where H^b and U^a refer to the residual enthalpy and residual internal energy, respectively, n_i is the mole number of component i, while a and b denote the adsorbed and bulk phases, respectively. The second part of the expression can be calculated during grand canonical simulations using the particle number fluctuations and the cross-correlation of potential energy and particle number fluctuations [27, 28]. If we assume an ideal gas adsorbate, the first part of the expression is equal to RT, where R is the gas constant.

Results and discussion

We tested some zeolite models given in the literature [13, 14] as well as our earlier model [11] for the equilibrium adsorption of water and carbon monoxide. Experimental data at T=373 K were taken from [6]. Simulation results and experimental data are compared in Table 2. Using the literature models, the reproduction of the experimental results is not satisfactory, especially for CO; in the case of model 1, the simulated data give values more than four times larger than the experimental results. Also, model 2 is definitely better for the polar component, i.e., it overestimates the experimental result for water by only 25%, but strongly underestimates the measured data for CO. Our previous model (model 3) overestimates the equilibrium amount of adsorption both for CO and H_2O, but to a lesser extent.

In the following we use a modified version of model 3 (see Table 1). After some test simulations, we found that

Table 2 Simulated and experimental data for the amount of adsorption (in mol/kg) with different models for zeolite NaA

Zeolite model	H_2O (T=373 K, p=6 kPa)	CO (T=373 K, p=101.3 kPa)
Model 1 [14]	14.75	1.58
Model 2 [13]	12.59	0.03
Model 3 [11]	11.52	0.52
Modified model 3	10.46	0.33
Experimental	10.1[a]	0.37[a]

[a] Experimental data are taken from Figs. 2–3 of Ref. [6] by digitalizing the curves

modification of the charge parameter of the Na^+ ion by only 0.1 (i.e., it is changed to 0.6) decreases the polarity of the zeolite framework sufficiently to reproduce satisfactorily the experimental results for the non-polar or weak polar gases (CO, H_2, and CH_4) as well as for water. The new charge parameter is not far from the value proposed by Lee et al. [12] for zeolite NaA obtained by using Huheey's electronegativity set and Sanderson's electronegativity equalization principle. To keep the transferability and neutrality of the model, an increase in the charge parameter of Al was also necessary. Table 2 illustrates that the modified model 3 represents reality much better than the other models.

Adsorption isotherms on zeolite NaA were calculated at temperatures where experimental data are available [6, 13, 29], and at T=338 K and 373 K, which were chosen for our mixture adsorption study (Fig. 1). We were able to reproduce the experimental data for water at T=373 K as well as for CO at T=338 K and 373 K satisfactorily. The comparison of the experimental and simulation results for CH_4 and H_2 shows that the zeolite model is appropriate for adsorption simulation with these substances too, even though the calculated amount of adsorption for CH_4 slightly overestimates the experimental data. The reproduction of the measured adsorption loadings for H_2 is pretty good over a wide range of pressure and, in the case of CH_4, the extent of overestimation is acceptable at pressures below atmospheric pressure. We expect, however, that the observed discrepancies between simulation and experiment for the non-polar components cannot cause significant errors in mixture adsorption data, where the adsorption of water is dominant [6, 10]. For the non-polar gases, the isotherms are in the Henry's law region (the amount of adsorption is a linear function of the bulk phase pressure), so in evaluation of the mixture adsorption data, the pure component's reference points can be obtained, if necessary, by simple linear interpolation. From the extent of adsorption loadings for pure components, it is obvious that electrostatic effects control the zeolite-adsorbate interactions, which means, e.g., that the amount of adsorption for pure H_2 and CH_4 should be rather low.

Figure 2 shows the calculated isosteric heat of adsorption data as a function of the bulk phase pressure at two different temperatures for H_2O, CO, H_2 and CH_4. The isosteric heat of adsorption is several times larger for

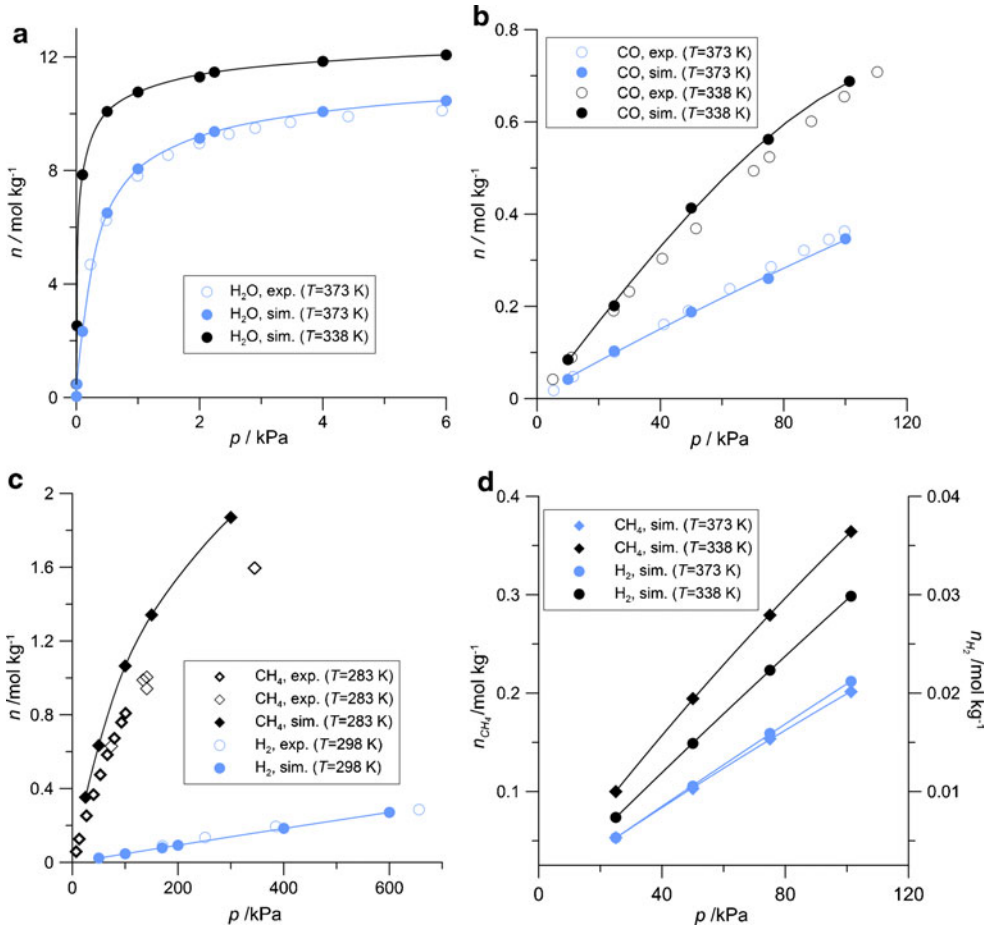

Fig. 1 Simulation results for the amount of adsorption (n) of **a** pure water, **b** carbon monoxide, **c** methane, and **d** hydrogen in zeolite NaA at T=338 K and 373 K and at other temperatures where experimental data for pure component are available [6, 13, 29]. *Closed symbols* simulation data, *open symbols* experimental data. The statistical uncertainties of the simulation results do not exceed the symbol size

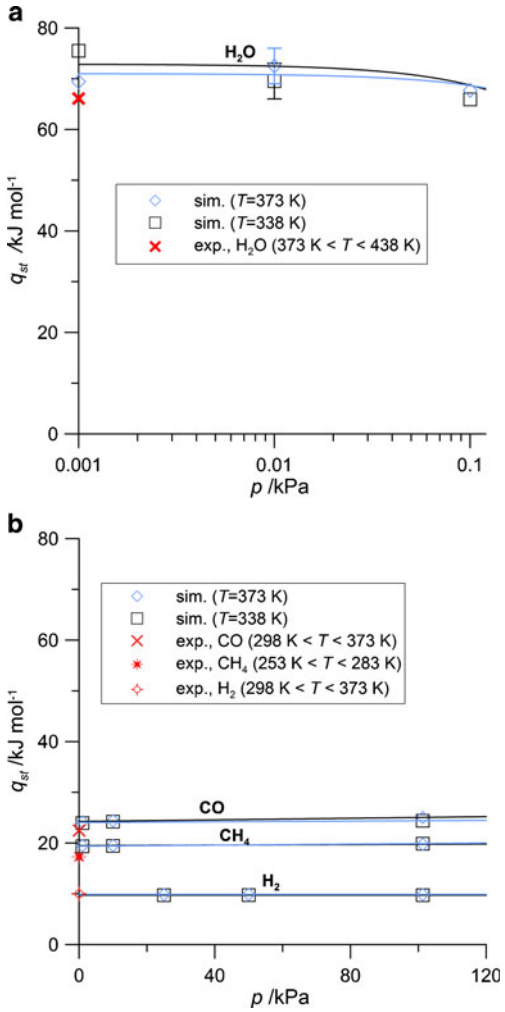

Fig. 2 Comparison of the simulated isosteric heat of adsorption results in zeolite NaA (q_{st}) with the corresponding experimental data for **a** pure water [6], and **b** carbon monoxide [6], methane [6, 29], and hydrogen [6, 13]

water than for the other substances. The data show the order $q_{st,H2O} > q_{st,CO} > q_{st,CH4} > q_{st,H2}$, which follows the expected tendency considering that the isosteric heat of adsorption extrapolated to zero coverage (see the intersection of the curves with the *y*-axis) is connected with the interaction energy between the zeolite framework and the adsorbate molecules. The higher isosteric heat of adsorption of CH_4 as compared to that of H_2 can be explained by the relatively large polarizability of the CH_4 molecules, which is implicitly taken into account in the attracting Lennard-Jones terms of the OPLS-AA model. On the other hand, the weakest zeolite-adsorbate attraction observed in the case of H_2 is due to the weak (though explicitly modeled) quadrupole moment and very low polarizability of the H_2 molecules. The agreement between simulation and experiment [6] is quite good for CO, H_2 and CH_4, where the pressure dependence of the heat of adsorption data is weak, and fairly good for water considering the uncertainty of the computation (and consequently, the extrapolation). Furthermore, one has to keep in mind that the experimental data shown in Fig. 2 [6, 13, 29] have been obtained from experiments performed over a wide range of temperature and represent mean values. According to the experiments, the isosteric heat of adsorption for water can decrease below 50 kJ mol^{-1} at a fully hydrated state, which is in good agreement with our simulation results at higher water pressure (data not shown), and indicates that the heat of adsorption data for water can vary in a wider range. Briefly, the results for the heat of adsorption support the adequacy of the models used in this study.

Figure 3 shows the relative difference between the results of the pure component adsorption and of the adsorption from binary mixtures with water, which is defined for a given component as $\Delta^n = \frac{n_{pure} - n_{mixture}}{n_{pure}}$. The total pressure of the bulk gas mixture was set to p= 101.3 kPa in all cases. Due to the high affinity of water for zeolite, the mixture adsorption data for water essentially does not differ from the corresponding pure component adsorption data, except at T=373 K and p_{H2O}=0.1 kPa, where the loading is relatively low for water. In other words, the presence of the non-polar (weakly polar) compound of the mixture does not affect the adsorption of water, demonstrating the excellent dehydration ability of zeolite NaA. On the other hand, the loadings of the non-polar (weakly polar) gases are influenced greatly by the presence of water. As the amount of adsorbed water in the zeolite increases with pressure, the amount of the other adsorbed components strongly decreases, and Δ^n converges to 1 for these components. The Δ^n curves of H_2, CO and CH_4 have two ranges with significantly differing slopes, below and above p_{H2O}=1 kPa, though this feature is less pronounced at T=338 K. The separation efficiency of the zeolite can be described by its equilibrium selectivity for water, which is defined for component i as $S_i = \frac{n^a_{H_2O}}{n^a_i} \cdot \frac{n^b_i}{n^b_{H_2O}}$. The selectivity curves show the above shape with two different ranges, especially for CO and CH_4. However, the behavior of the S_i values is partly the opposite of what is expected. Up to ~10.5 mol/kg adsorbed water (p_{H2O}<1 kPa at T=338 K and p_{H2O}<5 kPa at T=373 K) the selectivity order is the same, as can be expected from the affinity of the pure components, i.e., $S_{CO} < S_{CH4} < S_{H2}$, but as the adsorbed amount of water increases above ~10.5 mol/kg, the selectivity order becomes $S_{CO} < S_{H2} < S_{CH4}$. A lower adsorption loading of water leaves enough space for the adsorption of the second component and mostly the affinity of the pure gaseous components to the zeolite determines the loading. Therefore, the highest selectivity is related to

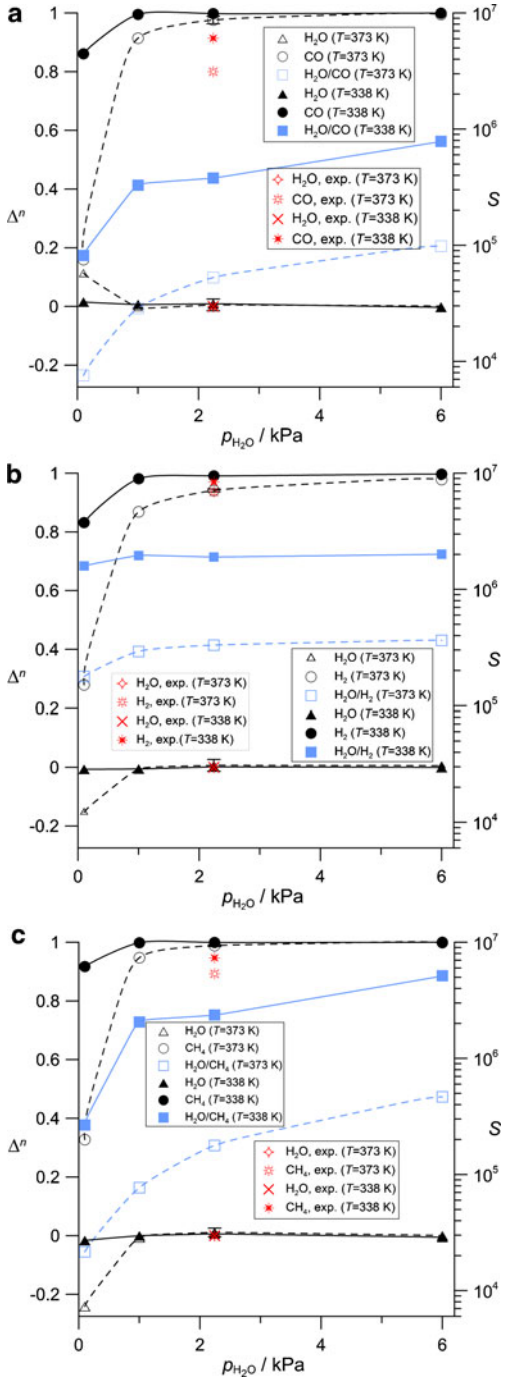

Fig. 3 **a**–**c** Relative difference of the adsorption coverages ($\Delta^n = \frac{n_{pure} - n_{mixture}}{n_{pure}}$, dark symbols) and selectivity of water to the other component (S, blue symbols) for adsorption from binary gas mixtures at p_{total}=101.3 kPa. Δ^n values calculated from experimental permeance data [6] are indicated for comparison

the weakest adsorption affinity. At the same time, at higher loadings of water with less free space inside the zeolite, the size effect can play a decisive role, and this favors adsorption of H_2 molecules. Similar results have been found experimentally by Zhu et al. [6] for permeation selectivities (permselectivities) in these systems at p_{H2O}= 2.24 kPa. (It should be noted that the selectivity can also be defined simply as $S'_i = \frac{n^a_{H_2O}}{n^a_i}$, and for the permselectivity, the adsorbed mole numbers are replaced by permeance data.) Although a direct comparison between these non-equilibrium experimental permselectivity data and our equilibrium simulation results cannot be made (we obtained substantially higher equilibrium adsorption selectivities), the basic similarities are apparent: the permeance of water in the binary mixtures was found practically the same as its pure component permeance, while the permeances of the non-polar (weakly polar) components decreased strongly in the presence of water.

The relative difference of the equilibrium selectivity values calculated at the two investigated temperatures is in the order of magnitude of 10, which is larger than would be expected from pure gas adsorption data. The values of the ideal selectivity $\frac{n^a_{H_2O}}{n^a_i}$, calculated from the pure gas adsorption data are several times smaller than the corresponding mixture selectivities (even if we simply take S'_i), and show only a slight increase (within a factor of 2) with temperature.

We have also simulated the adsorption from binary mixtures of CO and H_2. Again, the results underline the importance of the dipole moment of the adsorbate in the adsorption with this zeolite. Here, instead of water, CO will be the dominant molecule in the adsorbed phase (H_2O is replaced by CO in the above definition of selectivity). Figure 4 shows that the obtained Δ^n curves are mainly linear around zero, meaning that the number of adsorbed molecules does not differ significantly from the case of pure component adsorption. At the higher temperature, however, the amount of adsorbed CO increases only moderately with increasing CO partial pressure in the mixture. The calculated selectivities for CO are substan-

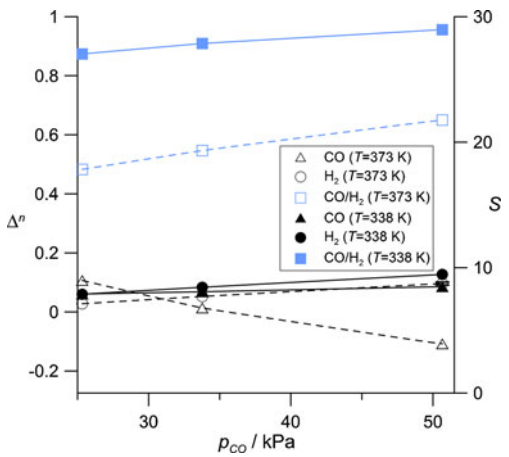

Fig. 4 Relative difference in adsorption coverages ($\Delta^n = \frac{n_{pure} - n_{mixture}}{n_{pure}}$, *dark symbols*) and selectivity of carbon monoxide to hydrogen (S, *blue symbols*) for adsorption from binary gas mixtures at p_{total}=101.3 kPa

Table 3 Simulation results for the amount of adsorption (n), relative difference (Δ^n %) and selectivity (S) for three- and four-component mixture adsorption at p_{total}=101.3 kPa (see text for definition of selectivity in this special case)

		$\frac{n}{\text{mmol·kg}^{-1}}$ (Δ^n%)				S/10^3
		H_2O	CO	H_2	CH_4	
$p_{H2O} : p_{CO} : p_{H2}$=2.24 : 49.53 : 49.53	373 K	9,326 (0.5%)	3.6 (98.1%)	0.60 (94.3%)		97.8
	338 K	11,390 (0.7%)	0.54 (99.9%)	0.13 (99.1%)		754
$p_{H2O} : p_{CO} : p_{H2}$=2.24 : 33.02 : 66.04	373 K	9,426 (−0.6%)	2.4 (99%)	0.77 (89%)		133
	338 K	11,448 (0.1%)	0.20 (~100%)	0.16 (98.4%)		1,430
$p_{H2O} : p_{CO} : p_{H2} : p_{CH4}$=0.1 : 25.3 : 50.6 : 25.3	373 K	2,695 (−16%)	69 (33%)	7.3 (31%)	36 (33%)	24.3
	338 K	7,815 (0.4%)	24 (88%)	2.6 (83%)	8.5 (91.5%)	226
$p_{H2O} : p_{CO} : p_{H2} : p_{CH4}$=2.24:33.02:33.02:33.02	373 K	9,328 (0.5%)	2.4 (98.1%)	0.41 (94.2%)	0.71 (99%)	116
	338 K	11,492 (−0.2%)	0.21 (99.9%)	0.08 (99.2%)	0.04 (~100%)	1,548
$p_{H2O} : p_{CO} : p_{H2} : p_{CH4}$=2.24:32.27:64.55:2.24	373 K	9,398 (−0.3%)	2.6 (98%)	0.83 (94%)	0.05 (99%)	118
	338 K	11,482 (−0.1%)	0.15 (99.9%)	0.13 (99.3%)	0.004 (~100%)	1,765
$p_{H2O} : p_{CO} : p_{H2} : p_{CH4}$=2.24:24.77:49.53:24.77	373 K	9,398 (−0.3%)	1.8 (98.2%)	0.59 (94.4%)	0.53 (99%)	141
	338 K	11,458 (0.07%)	0.12 (99.9%)	0.12 (99.2%)	0.04 (~100%)	1,812

tially lower than those obtained for water, but their temperature dependence again resembles the situation with water.

To approximate the real system of Fischer-Tropsch synthesis, we also studied multi-component adsorption. Here, a straightforward definition of the selectivity can be written as $S = \frac{n^a_{H_2O}}{\sum_{i\neq H_2O} n^a_i} \cdot \frac{\sum_{i\neq H_2O} n^b_i}{n^b_{H_2O}}$ (or $S = \frac{n^a_{CO}}{\sum_{i\neq CO} n^a_i} \cdot \frac{\sum_{i\neq CO} n^b_i}{n^b_{CO}}$). The results for the amount of adsorption and selectivity for water concerning three- and four-component mixtures (Table 3) confirm the results obtained for the binary mixtures with water, i.e., the adsorption of the gaseous components is suppressed strongly by water. As was already observed with the binary mixtures, the situation becomes slightly different at lower partial pressure of water; here water does not fill the zeolite framework completely and, consequently, the remaining components can, to some extent, keep their character in the adsorbed phase. In the case of the investigated anhydrous three-component mixtures (Table 4), the adsorption coverages are very similar to those obtained from pure component adsorption, with a maximum difference of 13%. For the equimolar mixture, the order of Δ^n values is the reverse of the order of pure gas affinities. The selectivity for the polar component CO is highest at the lowest CH_4 partial pressure, where the low adsorption affinity of H_2 is dominant. These systems behave similarly to the corresponding water-containing systems also in the sense that the selectivity for CO, though its values are much smaller, decreases with increasing temperature.

Conclusions

In this work, we propose a new parameter set for the potential model of zeolite NaA designed for the molecular simulation of adsorption. The new parameter set allows accurate determination of the adsorption loading of water and simple non-polar (weakly polar) gases in the zeolite, at least at temperatures slightly above room temperature.

Our simulation results confirm the experimental findings of Zhu et al. [6] and others [30], in general and in most details. As electrostatic effects dominate the interactions, zeolite NaA exhibits exceptional selectivity of water to non-polar or

Table 4 Simulation results for the amount of adsorption (n), relative difference of the adsorption coverages (Δ^n %) and selectivity (S) for three-component mixture adsorption of non-polar (weakly polar) gases at p_{total}=101.3 kPa (see text for the definition of selectivity in this special case)

		$\frac{n}{\text{mmol·kg}^{-1}}$ (Δ^n%)			S
		CO	H_2	CH_4	
$p_{CO} : p_{H2} : p_{CH4}$=33.77 : 33.77 : 33.77	373 K	132 (0.5%)	6.6 (8.1%)	66 (6.1%)	3.6
	338 K	264 (4.1%)	8.7 (13%)	118 (11%)	4.2
$p_{CO} : p_{H2} : p_{CH4}$=33.02 : 66.04 : 2.24	373 K	128 (2.0%)	13 (5.2%)	4.5 (5.1%)	15
	338 K	246 (8.6%)	18 (7.5%)	8.3 (7.2%)	19
$p_{CO} : p_{H2} : p_{CH4}$=25.325 : 50.65 : 25.325	373 K	95 (8.4%)	10 (5.1%)	51 (5.3%)	4.7
	338 K	205 (−0.3%)	13 (11%)	92 (8.9%)	5.8

weakly polar substances, and this feature can be attributed primarily to the high equilibrium adsorption affinity of the zeolite to water. Despite the fact that in non-equilibrium membrane permeation processes the selective character of the zeolite should also depend on the diffusivity of the fluid components, one can make good predictions of permeation tendencies from equilibrium adsorption data. In practical applications, the permeances of weakly polar gaseous components through zeolite NaA membranes are suppressed strongly by water, because the prevalent adsorption of water molecules blocks the windows of the zeolite cages, preventing the bypassing of the other components.

Acknowledgment This work was supported by the Hungarian Scientific Research Fund (Grant No. OTKA K75132).

References

1. Van Bekkum H, Flaningen EM, Jansen JC (eds) (1991) Introduction to zeolite science and practice. Elsevier, Amsterdam
2. Auerbach SM, Carrado KA, Dutta PK (eds) (2003) Handbook of zeolite science and technology. Dekker, New York
3. Okamoto K, Kita H, Horii K, Tanaka K, Kondo M (2001) Zeolite NaA membrane: preparation, single-gas permeation, and pervaporation and vapor permeation of water/organic liquid mixtures. Ind Eng Chem 40:163–175
4. Xu X, Yang W, Liu J, Chen X, Lin L, Stroh N, Brunner H (2000) Synthesis and gas permeation properties of an NaA zeolite membrane. Chem Commun 603–604
5. Aoki K, Kusakabe K, Morooka S (2000) Separation of gases with an A-type zeolite membrane. Ind Eng Chem 39:2245–2251
6. Zhu W, Gora L, van den Berg AWC, Kapteijn F, Jansen JC, Moulijn JA (2005) Water vapour separation from permanent gases by a zeolite-4A membrane. J Membrane Sci 253:57–66
7. Dry ME (2002) Fischer-Tropsch process: 1950–2000. Cat Today 71:227–241
8. Furukawa S, Goda K, Zhang Y, Nitta T (2004) Molecular simulation study on adsorption and diffusion behavior of ethanol/water molecules in NaA zeolite crystal. J Chem Eng Jpn 37:67–74
9. Kristóf T, Csányi É, Rutkai G, Merényi L (2006) Prediction of adsorption equilibria of water–methanol mixtures in zeolite NaA by molecular simulation. Mol Simul 32:869–875
10. Rutkai G, Csányi É, Kristóf T (2008) Prediction of adsorption and separation of water–alcohol mixtures with zeolite NaA. Microporous Mesoporous Mater 114:455–464
11. Csányi É, Kristóf T, Gy L (2009) Potential model development using quantum chemical information for molecular simulation of adsorption equilibria of water–methanol (ethanol)mixtures in zeolite NaA-4. J Phys Chem C 113:12225–12235
12. Lee SH, Moon GK, Choi SG, Kim HS (1994) Molecular dynamics simulation studies of zeolite-A. 3. Structure and dynamics of Na^+ ions and water molecules in a rigid zeolite-A. J Phys Chem 98:1561–1569
13. Akten ED, Siriwardane R, Sholl DS (2003) Monte Carlo simulation of single- and binary component adsorption of CO_2, N_2, and H_2 in Zeolite Na-4A. Energ Fuels 17:977–983
14. Calero S, Dubbeldam D, Krishna R, Smit B, Vlugt TJH, Denayer JFM, Martens JA, Maesen TLM (2004) Understanding the role of sodium during adsorption: a force field for alkenes in sodium-exchanged faujasites. J Am Chem Soc 126:11377–11386
15. Pluth JJ, Smith JV (1980) Accurate redetermination of crystal structure of dehydrated zeolite A. Absence of near zero coordination of sodium. Refinement of Si, Al-ordered superstructure. J Am Chem Soc 102:4704–4708
16. Berendsen HJC, Grigera JR, Straatsma TP (1987) The missing term in effective pair potentials. J Phys Chem 91:6269–6271
17. Straub JE, Karplus M (1991) Molecular dynamics study of the photodissociation of carbon monoxide from myoglobin: ligand dynamics in the first 10 ps. Chem Phys 158:221–248
18. Darkrim F, Aoufi A, Malbrunot P, Levesque D (2000) Hydrogen adsorption in the NaA zeolite: a comparison between numerical simulations and experiments. J Chem Phys 112:5991–5999
19. Kaminski G, Duffy E, Matsui T, Jorgensen W (1994) Free energies of hydration and pure liquid properties of hydrocarbons from the OPLS all-atom model. J Phys Chem 98:13077–13081
20. Song W, Rossky PJ, Maroncelli M (2003) Modelling alkane +perfluoroalkane interactions using all-atom potentials: failure of the usual combining rules. J Chem Phys 119:9145–9162
21. Waldman M, Hagler A (1993) New combining rules for rare gas van der Waals parameters. J Comput Chem 14:1077–1084
22. Gubbins KE, Quirke N (eds) (1997) Molecular simulation and industrial applications: methods, examples and prospects. Gordon and Breach, Amsterdam
23. Wolf D, Keblinski P, Phillpot SR, Eggebrecht J (1999) Exact method for the simulation of Coulombic systems by spherically truncated, pairwise r^{-1} summation. J Chem Phys 110:8254–8282
24. Demontis P, Spanu S, Suffritti GB (2001) Application of the Wolf method for the evaluation of Coulombic interactions to complex condensed matter systems: aluminosilicates and water. J Chem Phys 12:8267–8278
25. Kofke DA, Glandt ED (1988) Monte Carlo simulation of multicomponent equilibria in a semigrand canonical ensemble. Mol Phys 64:1105–1131
26. Jaramillo E, Chandross M (2005) Adsorption of small molecules in LTA zeolites. 1. NH3, CO2, and H2O in Zeolite 4A. J Phys Chem B 108:20155–20159
27. Nicholson D, Parsonage NG (1982) Computer simulation and the statistical mechanics of adsorption. Academic, London
28. Karavias F, Myers AL (1991) Isosteric heats of multicomponent adsorption: thermodynamics and computer simulations. Langmuir 7:3118–3126
29. Mohr RJ, Vorkapic D, Rao MB, Sircar S (1999) Pure and binary gas adsorption equilibria and kinetics of methane and nitrogen on 4A zeolite by isotope exchange technique. Adsorption 5:145–158
30. Nair S, Tsapatsis M (2003) Synthesis and properties of zeolitic membranes. In: Auerbach SM, Carrado KA, Dutta PK (eds) Handbook of zeolite science and technology. Dekker, New York, pp 869–921